Vibronic mechanism of high-T_c superconductivity

M. Tachiki
National Institute for Materials Science, 1-2-1 Sengen, Tsukuba, Ibaraki 305-0047, Japan

M. Machida
Center for Promotion of Computational Science and Engineering, Japan Atomic Energy Research Institute, 6-9-3 Higashi-Ueno, Taito-ku Tokyo 110-0015, Japan

T. Egami
Laboratory for Research on the Structure of Matter and Department of Material Science and Engineering, University of Pennsylvania, Philadelphia, Pennsylvania 19104

(Received 22 May 2002; revised manuscript received 19 September 2002; published 8 May 2003)

The dispersion of the in-plane Cu-O bond-stretching longitudinal optical phonon mode in the high-T_c superconducting cuprates shows strong softening with doping near the zone boundary. We suggest that it can be described with a negative electronic dielectric function that results in an overscreening of the intersite Coulomb interaction due to phonon-induced charge transfer and vibronic electron-phonon resonance. We propose that such a strong electron-phonon coupling of specific modes can form a basis for the phonon mechanism of high-temperature superconductivity. With the Eliashberg theory using the experimentally determined electron dispersion and dielectric function, we demonstrate the possibility of superconductivity with the order parameter of the $d_{k_x^2-k_y^2}$ symmetry and the transition temperature well in excess of 100 K.

DOI: 10.1103/PhysRevB.67.174506 PACS number(s): 74.72.−h, 74.20.Mn, 74.20.Rp

I. INTRODUCTION

The mechanism of the high-T_c superconductivity (HTSC) in the cuprates[1] remains elusive, in spite of extensive experimental and theoretical efforts. The majority view on the mechanism is to consider magnetic interactions as the main driving force.[2] However, the HTSC recently observed in MgB_2 (Ref. 3), graphite-sulfur composites (Ref. 4), and the *n*-type infinite-layer cuprate $Sr_{0.9}La_{0.1}CuO_2$ (Ref. 5) cannot be explained by magnetic mechanisms, since these compounds have small spin fluctuations in strong contrast to the cuprate superconductors. There is no reason to reject, then, the possibility that the HTSC in the cuprates also shares a similar nonmagnetic mechanism. In this paper we discuss a phonon mechanism of HTSC based upon the overscreening of the intersite Coulomb interaction, in light of recent experimental results on the cuprates. In this mechanism, unlike the BCS theory, the relevant phonons are not the long-wave acoustic phonons but the zone-edge optical phonons that induce intersite charge transfer.

The HTSC cuprates are doped Mott insulators. Even though the antiferromagnetism disappears with only about 2% of hole doping, strong antiferromagnetic spin fluctuations are observed by neutron scattering, nuclear magnetic resonance, and other methods. For this reason spin fluctuations have been considered to be the principal mechanism of the HTSC.[2,6–8] However, the intensity of spin fluctuations does not correlate, or even anticorrelate, with T_c as the hole concentration is changed. For instance the spin fluctuations measured by the nuclear relaxation of Cu in $Tl_2Ba_2CuO_{6-\delta}$ are the same for the sample with $T_c=85$ K and the overdoped sample with $T_c=0$.[9] Even when the composition is the same, the spin fluctuations of $La_{2-x}Ba_xCuO_4$ films prepared by epitaxial growth that have T_c of 47 K were found to be smaller than those of the bulk with T_c of 30 K.[10]

In this paper we propose a phonon mechanism based upon the anomalous screening of the intersite Coulomb interaction in a highly correlated electron system leading to strong pairing. This mechanism does not compete against the magnetic mechanism and could achieve HTSC alone or with a magnetic mechanism through synergetic effects. There is a large volume of literature showing a coupling of superconductivity to the lattice and phonon.[11–14] In particular the in-plane Cu-O bond-stretching LO phonon mode was observed by neutron inelastic scattering to show strong softening with doping near the zone boundary along the Cu-O bond direction.[11,15,16] This mode induces charge transfer between Cu and O, and thus couples strongly to the charge dynamics.[12,17,18] Recent neutron scattering measurements on $YBa_2Cu_3O_{7-\delta}$ (YBCO) suggest that the frequencies of the LO phonons are strongly softened with doping near the zone boundary, while the TO phonons are not.[19,20] Furthermore, no observation of the softening in the overdoped $La_{2-x}Sr_xCaCuO_4$ with almost zero T_c implies a systematic linkage between the phonon and superconductivity.[21] We propose that this occurs due to the phonon-induced charge transfer that results in the formation of a vibronic state[22] and a negative electronic dielectric function giving a main contribution to high-T_c superconductivity[21] as will be discussed in Sec. II.

Doped holes in the cuprate superconductors are highly correlated due to the on-site Coulomb interaction on Cu ions and resultant spin fluctuations. Holes are strongly renormalized due to these interactions, and as a result many physical properties of the cuprate oxides in the normal state show anomalous behavior. For example, a very unusual temperature dependence has been observed for the Hall[23] and Seebeck[24] coefficients and pseudegap excitations[25] have been observed above T_c. The quasiparticle band structure determined by angular-resolved photoemission is very different from those calculated with the local density approxima-

tion (LDA) due to the correlation effect.[26]

Because of these strong correlation effects, at present it is very difficult to calculate the electronic response function accurately from first principles. Instead, in the present paper we take a phenomenological approach based upon information obtained from the experimental data. We start with the model electronic band structure that agrees with the angle-resolved photoemission experiments[26] and estimate the effective interaction using the phonon dispersion determined by the inelastic neutron scattering experiments.[19,20,27] We then calculate the superconducting order parameter and the superconducting transition temperature on the basis of Eliashberg's formulation.[28] We show that the order parameter is of $d_{k_x^2-k_y^2}$-wave symmetry[29] and the superconducting transition temperature can exceed 200 K. Because of the *d* symmetry, the present phonon-mediated pairing mechanism does not compete against the spin-fluctuation mechanism. It is possible that both mechanisms operate in the cuprate, and the weight depends upon the doping level. The issue of the in-plane anisotropy in the phonon dispersion[19,20,27] and the effect of the possible local spin-charge stripe fluctuation will not be included in this paper and will be discussed in future publications.

In Sec. II we explain the idea of overscreening in the cuprate superconductors. In Sec. III we derive the equation with the charge kernel for the calculation of the order parameter and T_c. In Sec. IV we determine the energy band renormalized by the correlation effect by utilizing the experimental results of the angle-resolved photoemission and the dielectric function using the results of the neutron scattering measurements. In Sec. V we determine the kernel of the equation by using the model obtained in Sec. IV. We then numerically solve the equation and obtain the superconducting order parameter and estimate the value of the superconducting transition temperature. Section VI is devoted to a discussion.

II. OVERSCREENING MECHANISM AND THE EFFECTIVE INTERACTION BETWEEN CARRIERS

The starting point of this research is to recognize that the electron-phonon (e-p) interaction in such a strongly correlated electron system can be very different from that in conventional metals. In particular, since the carrier density in the cuprate superconductors is relatively low and the charge dynamics is strongly correlated with the spin dynamics, the medium-range Coulomb interaction is not fully screened. For instance the optical reflectivity does not saturate as in the standard Drude model even below the nominal plasma frequency.[30] Thus the system has strong dielectric interactions, unlike in the usual metals. In particular, since phonons modulate the covalent bonds, they induce charge transfer between ions and, therefore, local polarization. In this paper we suggest that this effect can be described with a negative electronic dielectric function.

Sometime ago Tachiki and Takahashi proposed an overscreening mechanism of phonon-mediated superconductivity.[31–33] To explain this mechanism let us consider a static case of the overscreening effect. We write a staggered external electric field as $D(\mathbf{q})$ and the induced staggered electric charge polarization as $P_{el}(\mathbf{q})$ and define the electronic charge susceptibility $\chi_{el}(\mathbf{q},0)$ by

$$4\pi P_{el}(\mathbf{q}) = \chi_{el}(\mathbf{q},0) D(\mathbf{q}). \tag{1}$$

Then, combining an electromagnetic relation $D(\mathbf{q}) = E(\mathbf{q}) + 4\pi P_{el}(\mathbf{q}) = \epsilon_{el}(\mathbf{q},0) E(\mathbf{q})$ with Eq. (1), we have

$$\frac{1}{\epsilon_{el}(\mathbf{q},0)} = 1 - \chi_{el}(\mathbf{q},0). \tag{2}$$

According to the Kramers-Krönig relation, we have

$$\chi_{el}(\mathbf{q},0) = 2\int_0^\infty d\omega \frac{1}{\omega} \rho_{el}(\mathbf{q},\omega), \tag{3}$$

where $\rho_{el}(\mathbf{q},\omega)$ is the spectral intensity of the electronic charge fluctuation given by

$$\rho_{el}(\mathbf{q},\omega) = -\frac{1}{\pi} \mathrm{Im}\left[\frac{1}{\epsilon_{el}(\mathbf{q},\omega)}\right]. \tag{4}$$

The spectral intensity is always positive and therefore we have an inequality from Eqs. (2)–(4),

$$\frac{1}{\epsilon_{el}(\mathbf{q},0)} \leqslant 1. \tag{5}$$

The inequality, Eq. (5), gives two regions $\epsilon_{el}(\mathbf{q},0) \geqslant 1$ and $\epsilon_{el}(\mathbf{q},0) \leqslant 0$. The former case is commonly seen for most materials, such as metals where $\epsilon(0,0)$ diverges positively, while the latter case corresponds to overscreening. Let us consider a positive test charge density $\rho_{test}(\mathbf{q})$. The test charge induces the screening charge density $\rho_{screen}(\mathbf{q})$ to reduce the energy of the system. The screening charge is always negative. Using this charge density, $1/\epsilon_{el}(\mathbf{q},0)$ is expressed as

$$\frac{1}{\epsilon_{el}(\mathbf{q},0)} = 1 - \frac{|\rho_{screen}(\mathbf{q})|}{\rho_{test}(\mathbf{q})}. \tag{6}$$

When $|\rho_{screen}(\mathbf{q})|$ is larger than $\rho_{test}(\mathbf{q})$ in Eq. (6), $1/\epsilon_{el}(\mathbf{q},0)$ is negative. This is the static overscreening effect.

The microscopic origin of the negative dielectric function may come from the following mechanism. The electric polarizability in covalent solids is qualitatively different from that in simple ionic crystals, since the covalency contributes to charge transfer between ions.[34] For instance in ferroelectric oxides the polarization due to charge transfer is as large as the ionic polarization. In $BaTiO_3$ the nominal valence of Ti is 4+ and the nominal *d* state configuration is d^0. But the *d* orbital of Ti and the *p* orbital of O are strongly hybridized. This charge transfer produces current, and thus electronic polarization, which adds to the ionic polarization, making the effective valence (Born effective charge) of Ti twice as large.[35,36] In undoped cuprate the same transfer occurs from the filled *p* level of O to the empty upper Hubbard band of Cu, contributory to an extra polarizability.

However, in a doped cuprate the situation is drastically different. The doped holes occupy mostly the oxygen *p* lev-

els, and they move either to the lower Hubbard band or the filled d_{z^2} orbital of Cu. Thus holes are transferred from O to Cu, creating the larger polarization, which adds to two ionic polarization. Then, Eqs. (1) and (2) give a negative dielectric function if $\chi_{el}(\mathbf{q},0)>1$. More detailed discussions of the lattice softening using Born effective charge will be given elsewhere.[37]

While the in-plane Cu-O bond-stretching LO phonon mode in the cuprates is strongly softened by doping, other phonon modes are relatively insensitive to the doping level.[11,15,16] Moreover, the softening is not observed in both the undoped and overdoped ones in which their superconducting transition temperatures almost diminish.[21] This fact suggests that the bond-stretching LO phonon and its softening are responsible for the superconductivity. Thus, for the sake of simplicity, we assume that the basic lattice dynamics is not affected by doping and the frequency of the bond-stretching mode is renormalized only by the interaction with charge fluctuations. This assumption allows us to write the frequency corresponding to the maximum value of the spectral intensity of the renormalized LO phonon in terms of the electronic dielectric function as[31,32]

$$\omega_{LO}^{*}(\mathbf{q})^2=\omega_{TO}(\mathbf{q})^2+\frac{\omega_{LO}(\mathbf{q})^2-\omega_{TO}(\mathbf{q})^2}{\epsilon_{el}'(\mathbf{q},\omega_{LO}^{*}(\mathbf{q}))}, \tag{7}$$

where ω_{TO} and ω_{LO} are, respectively, the bare TO and LO phonon frequencies in the insulating state, and $\epsilon_{el}'(\mathbf{q},\omega_{LO}^{*})$ is the real part of the electronic dielectric function. The experimental results that the frequency $\omega_{LO}^{*}(\mathbf{q})^2$ of the LO mode is lower than that of the TO mode. It indicates that the real part of $\epsilon_{el}(\mathbf{q},\omega_{LO}^{*}(\mathbf{q}))$ is negative. In $YBa_2Cu_3O_{6.95}$ (YBCO) and $La_{1.85}Sr_{0.15}CuO_4$ (LSCO) the inversion of the LO and TO frequencies is most pronounced in the region $q_x=0.25$–0.75 and $q_y=-0.2$–0.2, in units of $2\pi/a$, at ω_{LO}^{*}, being the measured LO frequency (approximately 55 meV for YBCO and 70 meV for LSCO).[16,19,20] We interpret this phenomenon as the consequence of the negative $\epsilon_{el}'(\mathbf{q},\omega_{LO}^{*}(\mathbf{q}))$.

The quasiparticles are renormalized due to the on-site Coulomb interaction as mentioned in the Introduction. The interaction increases the effective mass of the quasiparticles, but does not change the charge e of the particles. Therefore, the effective potential acting between quasi-particles $\mathbf{k}$ and $\mathbf{k}'$ is written as

$$V_{eff}(\mathbf{q},\omega)=\frac{V(\mathbf{q})}{\epsilon(\mathbf{q},\omega)}, \tag{8}$$

where $V(\mathbf{q})$ is the bare Coulomb interaction and $\mathbf{q}$ is $\mathbf{k}-\mathbf{k}'$. Therefore with the normal screening the effective potential is always smaller than the bare potential. However, in the case of overscreening $\epsilon_{el(\mathbf{q},\omega)}'$ can be negative, and thus $\epsilon_{el}'(\mathbf{q},\omega)$ contributes to the effective interaction and works to enhance the phonon mediated attractive interaction as seen in Sec. III. Since the overscreening effect comes from various kinds of the correlation effect, $\epsilon(\mathbf{q},\omega)$ is a complicated function of charge, spin, and lattice. This effect is the core of the present mechanism.

Consequently the attractive interaction should exist between the quasiparticles with $\mathbf{k}$ and $\mathbf{k}'$ when $\mathbf{q}=\mathbf{k}-\mathbf{k}'$ is in the $\mathbf{q}$ regions where the phonon softening occurs, as seen in Eq. (7). In addition the negative electronic dielectric function turns the repulsive electron-electron Coulomb interaction into attraction, as in the so-called negative-U mechanism, and can promote pairing.

III. FORMULATION FOR SUPERCONDUCTING PAIRING

In this section we derive the equation to calculate the symmetry of the superconducting order parameter and T_c, using the effective interaction, Eq. (8).[31,32] In the effective interaction, the dynamical dielectric function $\epsilon(\mathbf{q},\omega)$ is given by the sum of the electronic dielectric function $\epsilon_{el}(\mathbf{q},\omega)$ and the ionic dielectric function $\epsilon_{ion}(\mathbf{q},\omega)$ as

$$\epsilon(\mathbf{q},\omega)=\epsilon_{el}(\mathbf{q},\omega)+\epsilon_{ion}(\mathbf{q},\omega)-1. \tag{9}$$

A minus unity on the right hand side of Eq. (9) comes from the fact that all the dielectric functions should be unity at the high-frequency limit. We express the ionic dielectric function in a conventional form

$$\epsilon_{ion}(\mathbf{q},\omega)=\frac{\omega^2-\omega_{LO}^2}{\omega^2-\omega_{TO}^2}, \tag{10}$$

ω_{LO} and ω_{TO} being, respectively, the frequencies of the bare longitudinal and transverse optical phonons in the insulating state. For simplicity, we consider one optical phonon mode, which seems to be most relevant to the superconductivity, and assume that it is dispersionless in the unrenormalized state. The spectral intensity function of total charge fluctuations is expressed by using Eqs. (4),(9), and (10) as

$$\begin{aligned}\rho(\mathbf{q},\omega)&=-\frac{1}{\pi}\mathrm{Im}\left[\frac{1}{\epsilon(\mathbf{q},\omega)}\right]\\&=-\frac{1}{\pi}\mathrm{Im}\left[\frac{1}{\epsilon_{el}(\mathbf{q},\omega)}\right]+\frac{\omega_{LO}^2(\mathbf{q})-\omega_{TO}^2}{\epsilon_{el}(\mathbf{q},\omega_{LO}^{*})^2}\,\delta(\omega^2-\omega_{LO}^{*2}),\end{aligned} \tag{11}$$

where the first term on the right-hand side of Eq. (11) is the electronic spectral intensity $\rho_{el}(\mathbf{q},\omega)$, and $\omega_{LO}^{*}(\mathbf{q})$ is the LO phonon frequency renormalized by charge fluctuations and is given by Eq. (1). If we use the spectral representation for $1/\epsilon(\mathbf{q},\omega)$, the effective interaction, Eq. (8), is written as

$$\begin{aligned}V_{eff}(\mathbf{q},\omega)&=V(\mathbf{q})/\epsilon(\mathbf{q},\omega)\\&=V(\mathbf{q})\left[1-2\int_0^{\infty}d\Omega\,\frac{\Omega\rho(\mathbf{q},\Omega)}{\Omega^2-(\omega+i\delta)^2}\right].\end{aligned} \tag{12}$$

Using Eq. (12) we set up the Eliashberg equation linearized with respect to the gap function $\Delta(\mathbf{k},i\omega)$ as

$$\Delta(\mathbf{k},i\omega_n)=-T\sum_{\ell}\sum_{\mathbf{k}'}V_{eff}(\mathbf{k}-\mathbf{k}',i\omega_n-i\omega_\ell)\frac{\Delta(\mathbf{k}',\omega_\ell)}{\xi_{\mathbf{k}'}^2+\omega_\ell^2}, \tag{13}$$

where $\omega \equiv (2n+1)\pi T$, with n being integer, and ξ_k is the quasiparticle energy measured from the Fermi level. We use an approximation that the damping of the quasiparticles is neglected. However, the modification of the band structure due to the correlation effect is taken into account by using the model band structure determined by the experimental results of angle-resolved photoemmision. If we introduce the pair function defined by

$$F(\mathbf{k}, i\omega_n) = \Delta(\mathbf{k}, i\omega_n)/(\omega_n^2 + \xi_{\mathbf{k}}^2), \tag{14}$$

Eq. (13) is rewritten as

$$F(\mathbf{k}, i\omega_n) = -\frac{1}{(\omega_n^2+\xi_{\mathbf{k}}^2)} T \sum_{\ell} \sum_{\mathbf{k}'} V_{eff}(\mathbf{k}-\mathbf{k}', i\omega_n - i\omega_\ell) \times F(\mathbf{k}', i\omega_\ell). \tag{15}$$

We then introduce again a function $f(k,v)$ (Ref. 38) defined by

$$F(\mathbf{k}, i\omega_n) = 2\int_0^\infty dv \, \frac{v f(\mathbf{k}, v)}{\omega_n^2 + v^2} \tag{16}$$

and also

$$\Phi(\mathbf{k}) = 2|\xi_{\mathbf{k}}| \int_0^\infty dv \, f(\mathbf{k}, v). \tag{17}$$

Then, from Eqs. (14) and (16) we can show that $\Phi(\mathbf{k})$ is equal to $\mathrm{Re}\,\Delta(\mathbf{k}, \xi_k)$ to a good approximation. The equation for $\Phi(\mathbf{k})$ is obtained substituting Eqs. (16) and (17) for Eq. (15) as

$$\Phi(\mathbf{k}) = -\sum_{\mathbf{k}} K(\mathbf{k}, \mathbf{k}') \frac{\tanh \xi_{\mathbf{k}'}/2T}{2\xi_{\mathbf{k}'}} \Phi(\mathbf{k}'). \tag{18}$$

In Eq. (18), the kernel $K(\mathbf{k}, \mathbf{k}')$ is given by

$$K(\mathbf{k}, \mathbf{k}') = v(\mathbf{k}-\mathbf{k}') \left[1 - 2\int_0^\infty d\Omega \, \frac{\rho(\mathbf{k}-\mathbf{k}', \Omega)}{\Omega + |\xi_{\mathbf{k}}| + |\xi_{\mathbf{k}'}|} \right]. \tag{19}$$

If we insert Eq. (11) for $\rho(\mathbf{q}, \omega)$ into Eq. (19) and use the Kramers-Kronig relation for $\mathrm{Im}[1/\epsilon_{el}(\mathbf{q}, \omega)]$ in $\rho_{el}(\mathbf{q}, \omega)$, the kernel, Eq. (19), is written as

$$K(\mathbf{k}, \mathbf{k}') = v(\mathbf{k}-\mathbf{k}') \left[\frac{1}{\epsilon_{el}(\mathbf{q}, 0)} + 2\int_0^\infty d\Omega \, \frac{|\xi_{\mathbf{k}}| + |\xi_{\mathbf{k}'}|}{\Omega(\Omega + |\xi_{\mathbf{k}}| + |\xi_{\mathbf{k}'}|} \rho_{el}(\mathbf{q}, \Omega) - \frac{1}{\epsilon_{el}(\mathbf{q}, \omega_{LO}^*(\mathbf{q}))} \frac{\omega_{LO}^{*2}(\mathbf{q}) - \omega_{TO}^2}{\omega_{LO}^*(\mathbf{q})[\omega_{LO}^*(\mathbf{q}) + |\xi_k| + |\xi_{k'}|]} \right]. \tag{20}$$

Roughly speaking, on the right-hand side of Eq. (20) the first two terms are the electronic contribution and the third term is the phonon contribution. However, the electronic contribution is mixed also in the third term as seen in Eq. (20). Therefore, the kernel has a vibronic nature.

The spectral intensity $\rho(\mathbf{q}, \omega)$ is approximately written around ω being $\omega_{LO}^*(\mathbf{q})$ (Ref. 31) as

$$\rho(\mathbf{q}, \omega) = \frac{1}{\epsilon_{el}'(\mathbf{q}, \omega_{LO}^*(\mathbf{q}))^2} \frac{\omega_{LO}^2 - \omega_{TO}^2}{2\pi\omega_{LO}^*(\mathbf{q})} \frac{\Delta(\mathbf{q})}{[\omega - \omega_{LO}^*(\mathbf{q}^2 + \Delta^2(\mathbf{q})}, \tag{21}$$

with

$$\Delta(\mathbf{q}) = \frac{\epsilon_{el}''(\mathbf{q}, \omega_{LO}^*)}{\epsilon_{el}'(\mathbf{q}, \omega_{LO}^*(\mathbf{q}))^2} \frac{\omega_{LO}^2(\mathbf{q}) - \omega_{TO}^2(\mathbf{q})}{2\omega_{LO}^*(\mathbf{q})}. \tag{22}$$

In Eq. (22), $\epsilon_{el}''(\mathbf{q}, \omega_{LO}^*)$ is the imaginary part of the electronic dielectric function. $\Delta(\mathbf{q})$ is the half width in the frequency ω_{LO}^* of the spectral function. If we use the experimental frequency values in Fig. 2, $\epsilon_{el}'(\mathbf{q}, \omega_{LO}^*)$ is given -0.068 from Eq. (7) for YBCO. Using this value, Eq. (22), and the neutron scattering experimental value of $\Delta(\mathbf{q})$ ~ 2 meV, we obtain $\epsilon_{el}''(\mathbf{q}, \omega_{LO}^*)$ to be 0.0069. Therefore, we can approximate $\epsilon_{el}(\mathbf{q}, \omega_{LO}^*(\mathbf{q}))$ by $\epsilon_{el}'(\mathbf{q}, \omega_{LO}^*)$, while we can see that the damping on the low-frequency charge fluctuation is very weak.

In conventional systems with $\epsilon_{el}'(\mathbf{q}, \omega) \geqslant 1$ the third term in Eq. (20) cannot be enhanced. However, when $\epsilon_{el}'(\mathbf{q}, \omega) < 0$ and its absolute value is small, the phonon contribution can be strongly enhanced, as seen from Eq. (20). The strong softening of $\omega_{LO}^*(\mathbf{q})$ also enhances the third term. Thus, it is found that the extent of the softening correlates with the superconducting transition temperature in the present mechanism. In fact, the remarkable softening occurs only in optimally doped cuprates.[21]

IV. QUASIPARTICLE BAND STRUCTURE AND ELECTRONIC DIELECTRIC FUNCTION IN CUPRATE SUPERCONDUCTORS

In this section, the quasiparticle band structure and the dielectric function are determined by utilizing the experimental data of the angle-resolved photoemission and inelastic neutron scattering. The results will be used in the following section in calculating the symmetry of the superconducting order parameter and the superconducting transition temperature with the Eliashberg equation.

A. Quasiparticle band structure

We assume that the layers responsible for the high-T_c superconductivity are mainly the CuO_2 layers. Then, we construct the energy band of the CuO_2 layer (the a-b plane) so as to agree with the results of the angle-resolved photoemission spectroscopy (ARPES).[26,39] The band structure is almost universal for all cuprate superconductors with optimum doping.[26] The angle-resolved photoemission[39] and the calcu-

lation including the correlation effect[40] show that the energy band in the cuprate superconductors is very flat in the region of $k_x(k_y)=0.25$–0.75 in units of $2\pi/a$, at 10–30 meV below the Fermi level. Hereafter, we express the wave number in units of $2\pi/a$. This is the region where the superconducting gap is the largest, and the kink in dispersion, which is interpreted as an evidence of strong electron-phonon coupling,[14] is most conspicuous. Therefore it is reasonable to expect that the charge fluctuation created by quasiparticles on the flat-band is very low in energy, comparable to the optical phonon frequency. Then, the quasiparticles and phonons can be highly mixed, and this system consequently becomes vibronic. As a result the quasiparticle-phonon interaction is highly enhanced, as will be shown in Secs. III and V.

The band structure with the flat regions along the k_x and k_y axes which originate from the strong renormalization effect[40] is reproduced by the following function:

$$\begin{aligned}\xi_k = C_B[&t_0 + 2t_1(\cos 2\pi k_x + \cos 2\pi k_y) \\ &+ 4t_2 \cos 2\pi k_x \cos 2\pi k_y + 2t_3(\cos 4\pi k_x + \cos 4\pi k_y)] \\ &+ F_B(E_f - \omega_g) - E_f, \end{aligned} \tag{23}$$

where t_0, t_1, t_2, and t_3 are, respectively, 0.0, -0.2, 0.0, and -0.04, E_f is -0.11, and ω_g is from 0.01 to 0.03 in units of eV. In this equation, if the second term is dropped, the equation approximately coincides with that of the usual LDA band calculation.[41] The second term is required to reproduce the flat regions mentioned above. The function F_B is given by

$$\begin{aligned}F_B = W_x&\left(1 + \frac{1}{2}\tanh[(k_x - k_L)/\lambda_L] - \frac{1}{2}\tanh[(k_x + k_L)/\lambda_L]\right) \\ &+ W_y\left(1 + \frac{1}{2}\tanh[(k_y - k_L)/\lambda_L]\right. \\ &\left. - \frac{1}{2}\tanh[(k_y + k_L)/\lambda_L]\right), \end{aligned} \tag{24}$$

with

$$W_x = -\frac{1}{2}\tanh[(k_y - k_T)/\lambda_T] + \frac{1}{2}\tanh[(k_y + k_T)/\lambda_T], \tag{25}$$

$$W_y = -\frac{1}{2}\tanh[(k_y - k_T)/\lambda_T] + \frac{1}{2}\tanh[(k_y + k_T)/\lambda_T], \tag{26}$$

where k_L, k_T, and $\lambda_L = \lambda_T$ are parameters to control the extent of the flat regions. A function F_B has sizable values only in certain regions near the k_x and k_y axes. For C_B and F_B, a constraint $C_B + F_B = 1$ is imposed. Figure 1 shows the band structure calculated by using Eqs. (23)–(26) where k_L, k_T, and λ_L $(=\lambda_T)$ are, respectively, taken as 0.16, 0.15, and 0.2 in units of $2\pi/a$. The values above are chosen to reproduce the ARPES data for the optimally doped YBCO.

As seen in the inset (a) of Fig. 1 the flat regions of the energy bands are located along the k_x axis and extend from $(-0.5, 0)$ to $(-0.25, 0)$ and from $(0.25, 0)$ to $(0.50, 0)$, and similarly along the k_y axis. The behavior has been observed in optimally doped YBCO and LSCO by ARPES.[26,39] The energy of the flatband is from 10 meV to 30 meV below the Fermi level.[26] In Fig. 1, ω_g is chosen to be 18 meV below the Fermi level. These flat regions mainly originate from the correlation effect reflecting the electron scattering due to spin fluctuations.[40] In these regions the effective masses and the damping constants of the quasiparticles are very large. On the other hand, the energy band in the directions from the (0, 0) point to the (0.5, 0.5), (0.5, -0.5), (-0.5, 0.5), (-0.5, -0.5) points is not much affected by the correlation effects and the dispersion of the electronic energy band structure is usual as seen in the inset (b) of Fig. 1.

B. Dielectric function

Recent inelastic neutron scattering measurements on the optimally doped YBCO show that the frequencies of the LO and TO phonons of the Cu-O bond-stretching LO mode are inverted in the region of $q_x = 0.25$–0.5,[16,19,20,27] suggesting that $\epsilon'_{el}(q_x, \omega^*)$ in this region is negative according to Eq. (7) and the LO phonons are overscreened by charge fluctuations (see Fig. 2). On the other hand, both the undoped and overdoped cuprates do not show such an inversion (see Fig. 2).[21] It was also observed that the phonon dispersions are anisotropic along the a and b axes. In this paper, however, we neglect this anisotropy for the sake of simplicity and assume the tetragonal symmetry of the crystal, skipping details of the dispersion. The effect of the anisotropy will be discussed elsewhere.[42] We then assume that the dielectric anomalies occur in the shaded regions as shown in Fig. 3. We divide the **q** space into two regions, region II, the shaded area in Fig. 3, where anomalous dielectric behavior is observed, and region I, which is outside region II with normal dielectric behavior. In region I we assume the Thomas-Fermi type of screenings of the Coulomb interaction due to quasiparticles, since the plasma frequency is much higher than kT_c and the frequency of the optical phonons. Then, the inverse of the dielectric function in region I is expressed as

$$\frac{1}{\epsilon_{el}(\mathbf{q}, \omega)} \approx \frac{1}{\epsilon_{el}(\mathbf{q}, 0)} = \frac{q^2}{q^2 + q_{TF}^2}, \tag{27}$$

where q_{TF} is the Thomas-Fermi wave number and its value is an order of unity in the units of the reciprocal lattice constant for the optimally doped cuprate superconductors.[43] In this region, we note that the repulsive interaction by the spin fluctuation scattering is located at (0.5,0.5),[6–8] but in the present paper this interaction is neglected in order to concentrate on the dielectric charge channel. The repulsive interaction actually exists, but for the moment we presume that the main pairing contribution arises from the dielectric charge channel. In region II, we assume that the excitation frequency of the electronic charge fluctuations is much lower than the plasma frequency for **q** in the region. The existence of such a low energy charge fluctuation due to anomalous

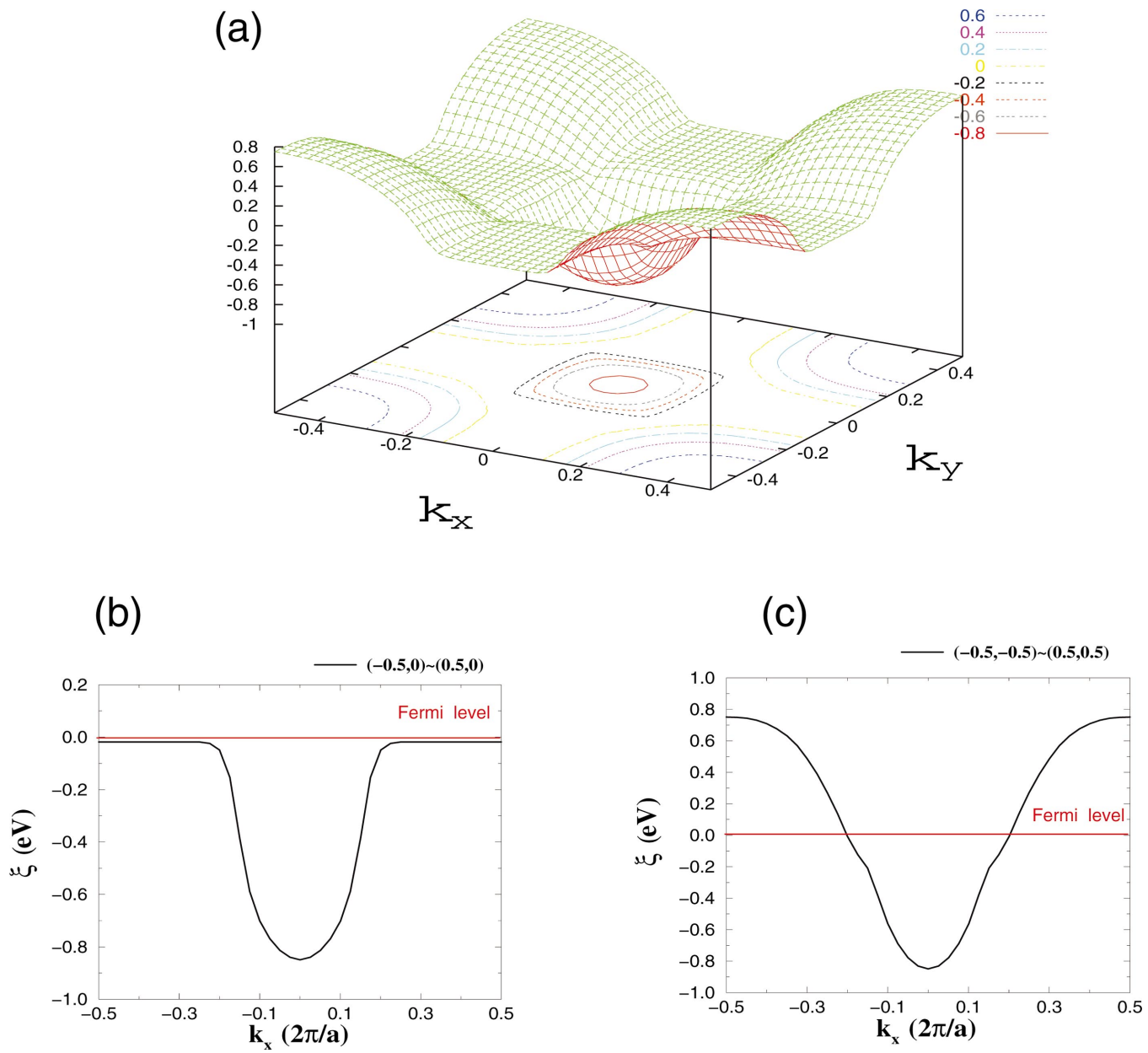

FIG. 1. (Color) A typical example of electronic band structure for calculating T_c and the superconducting order parameter. The parameters required for giving the flatband region as seen in this figure are $k_L=0.16$, $k_T=0.15$, and $\lambda_L(\lambda_T)=0.2$ in units of $2\pi/a$, and the parameter for the depth of the flat region $\omega_g=0.018$ eV. The z axis indicates the energy of quasiparticles in units of 1 eV. (a) The cut of the band structure from $(-0.5,0)$ to $(0.5,0)$. The Fermi level is displayed. (b) The cut from $(-0.5,-0.5)$ to $(0.5,0.5)$.

electronic structures has been suggested in Ref. 44. The existence of the low-frequency charge excitation is a necessary condition for the appearance of the negative dielectric function. Then, in region II, for the inverse of the dielectric function for positive low frequencies, we assume the following one pole approximation:

$$\frac{1}{\epsilon_{el}(\mathbf{q},\omega)} \approx A\left(\frac{1}{\omega-\omega_0+i\gamma}\right), \tag{28}$$

where A, ω_0, and γ are, respectively, the amplitude, the frequency of the charge fluctuation density maximum, and the damping constant. From Eq. (28), A is given by

$$A=\frac{\omega-\omega_0}{\epsilon'_{el}(\mathbf{q},\omega)}. \tag{29}$$

Using Eq. (7) and the experimental values of the frequencies shown in Fig. 2 we estimate $\epsilon'_{el}(\mathbf{q},\omega^*_{LO})$ to be -0.068. The value of ω_0 is much lower than the plasma frequency ($\hbar\omega_p=0.8$ eV) measured at small $\mathbf{q}$ by the optical measurement.[30,43] Inserting the value of ω^*_{LO} for ω into Eq. (29), we obtain A to be from 132 meV if $\hbar\omega_0$ is assumed to be 64 meV. The value of A linearly increases with ω_0. However, we note that Eq. (28) is valid only in the vicinity of the

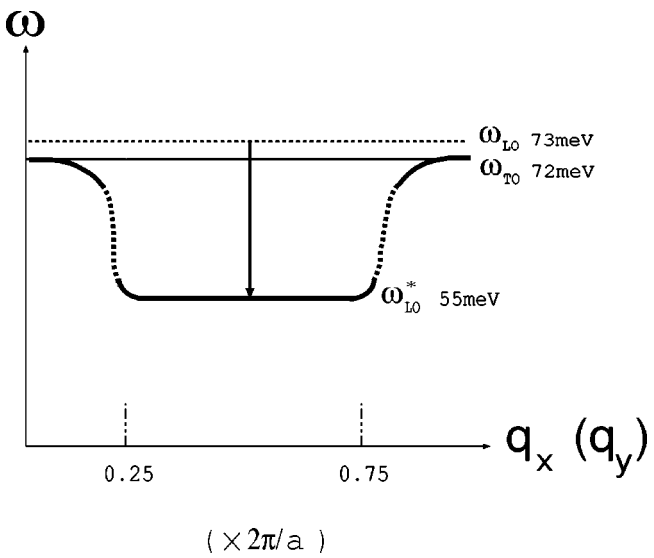

FIG. 2. The schematic view of the difference in the energy levels of the breathing LO and TO phonons between undoped and doped cuprates for YBCO. In the undoped state, the LO and TO branches are dispersionless and are at 73 and 72 meV, respectively, while in the doped state the LO level goes down to 55 meV in the range from 0.25 to 0.75 in q_x and q_y directions although the TO level still remains dispersionless. The $q_x(q_y)$ is measured in units of π/a.

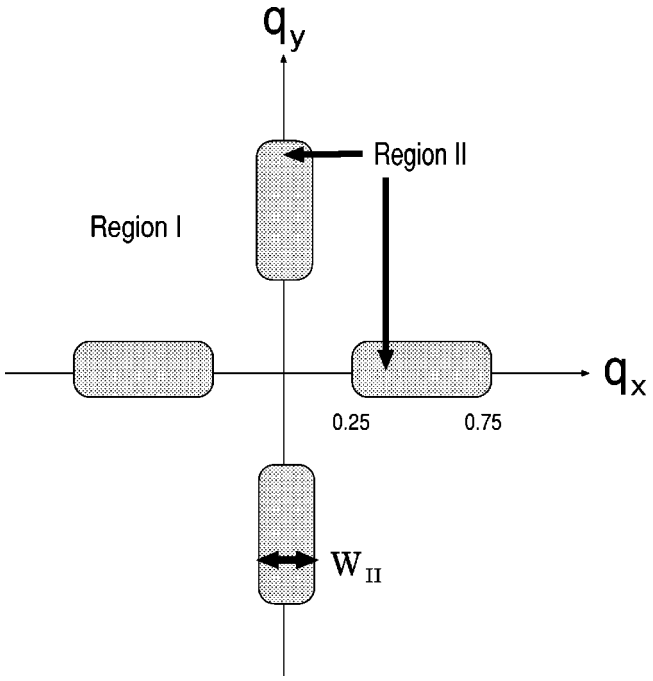

FIG. 3. Schematic view of the division into region I and region II (the hatched region) in the space of the scattering wave number between two quasiparticles. In region I, the Coulomb interaction is screened as in a usual metal, while anomalous screening occurs in region II due to strong correlation effects. Thus, for the dielectric function, the expression for Thomas-Fermi type of screening is used in region I, while the one obtained from the experimental result (neutron scattering) is used for region II.

low charge excitation energy $\hbar\omega_0$. Using the value of A and $\epsilon''_{el}(\mathbf{q},\omega^*_{LO})$ calculated from Eq. (22), we obtain γ to be ~ 1 meV.

V. SUPERCONDUCTING GAP SYMMETRY AND T_c

In the previous section, we constructed the model electronic band structure and derived the dielectric function based on the recent experimental results. In this section, we determine the kernel, Eq. (20), using the experimental values given in Sec. VI and calculate T_c and the superconducting gap function by solving Eq. (18).

Let us first concentrate on the kernel function in Eq. (20). The first term in the brackets in Eq. (20) represents the static dielectric function. It gives the repulsive contribution in region I in Fig. 3, while the term becomes negative, causing an attractive interaction in region II. The term in region II is determined by extrapolating the real part of the dielectric function, Eq. (27), to zero frequency as

$$\frac{1}{\epsilon'_{el}(\mathbf{q},0)} = -A\frac{1}{\omega_0}, \tag{30}$$

where Eq. (28) is used. At this moment we do not have exact information on the value of ω_0. However, since a strong phonon-induced charge transfer is expected, the value of ω_0 must be close to the value of ω^*_{LO}, 55 meV. We thus assume the value of ω_0 to be 64 meV. Thus, $1/\epsilon'_{el}(\mathbf{q},0)$ is given to be ~ 2. The second term always vanishes on the Fermi surface since $\xi_k = \xi_{k'} = 0$ on the surface, but it gives a repulsive interaction in finite energy ranges from the Fermi level. It is found from the numerical calculations that the contribution of the second term dominates over the attractive first and third terms when ξ_k and $\xi_{k'}$ are sufficiently far from the Fermi level.[42] The third term gives the attractive interaction originating from the optical phonons which is renormalized by the electronic dielectric function. This term is strongly enhanced due to overscreening in region II. Such a strong enhancement in region II can be understood by rewriting and comparing the third term for regions I and II, respectively, as follows:

$$\frac{q^2}{q^2+q_{TF}^2}\,\frac{{\omega^*_{LO}}^2(\mathbf{q})-\omega_{TO}^2}{{\omega^*_{LO}}^2(\mathbf{q})} \quad \text{for region I} \tag{31}$$

and

$$\frac{1}{\epsilon'_{el}(\mathbf{q},\omega^*_{LO})}\,\frac{{\omega^*_{LO}}^2(\mathbf{q})-\omega_{TO}^2}{{\omega^*_{LO}}^2(\mathbf{q})} \quad \text{for region II,} \tag{32}$$

where both ξ_k and ξ'_k in the third term are set to zero to compare their contributions on the Fermi surface. If q is set to 0.5 for both equations, a reasonable value of q_{TF} is employed and the observed values ω^*_{LO} in both regions are substituted; it is found that the contribution in region II becomes more than about 100 times larger than that in region I. The reason is explained as follows. In region II, the amplitude of $1/\epsilon^*_{el}(\mathbf{q},\omega)$ almost diverges negatively at ω_0. Therefore, the

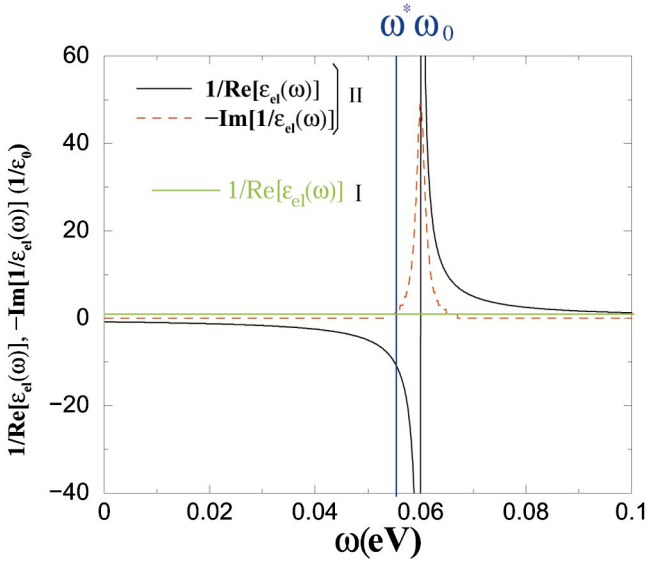

FIG. 4. (Color) The ω dependences of $1/\epsilon'_{el}(\omega)$ in regions I and II and $-\mathrm{Im}[1/\epsilon_{el}(\omega)]$ in the region II. The solid green line represents $1/\epsilon'_{el}(\omega)$ in region I, while the solid black and the dashed red lines stand for $1/\epsilon'_{el}(\omega)$ and $-\mathrm{Im}[1/\epsilon_{el}(\omega)]$, respectively. In region I there is no characteristic peak structure within the frequency range ($0 \approx 0.1$ eV) because its peak is located at the high-plasma-frequency range (≈ 0.8 eV). On the other hand, in region II the fluctuation peak lies at ω_0 as shown in this figure.

amplitude of $1/\epsilon'_{el}(\mathbf{q},\omega)$ at $\omega \approx \omega^*_{LO}$ still remains very large as shown in Fig. 4. The value of Eq. (32) is estimated to be 10.7. On the contrary such a anomalous structure does not exist in the vicinity of the phonon frequency in region I and the amplitude of $1/\epsilon'_{el}(\mathbf{q},\omega)$ remains as normal values as in conventional metals. These different features for regions I and II are seen in Fig. 4.

Thus, the electric overscreening effect is found to enhance the phonon contribution strongly and to give a strong attractive interaction. In fact, comparison between the first and third term contributions in region II for the quasiparticles on the Fermi surface tells us that the third term contribution is 10 times larger than the first term in this case. This result indicates that the electron-phonon interaction enhanced by overscreening could be the main pairing interaction in the cuprate superconductors.

Next, we actually calculate T_c and the k dependence of the gap function by solving Eq. (18). For this purpose we use the following technique. We introduce an eigenvalue equation with an eigenvalue $\lambda(T)$,[31,32]

$$\lambda(T)\Phi(\mathbf{k}) = -\sum_{\mathbf{k}'} K(\mathbf{k},\mathbf{k}')\frac{\tanh(\xi_{\mathbf{k}'}/2T)}{2\xi_{\mathbf{k}'}}\Phi(\mathbf{k}'). \quad (33)$$

We numerically calculate $\lambda(T)$ as a function of temperature T. The temperature satisfying $\lambda(T)=1$ corresponds to the superconducting transition temperature T_c. In addition, since $\Phi(k)$ corresponds to the superconducting gap function, the k dependence of $\Phi(k)$ gives the superconducting gap symmetry. However, it should be noted that the amplitude of the gap function is meaningless since the equation is a linearized equation which is valid only in the close vicinity of T_c.

A typical example of the superconducting gap function is shown in Fig. 5, where we use 13 meV for ω_g in Eq. (23) and 64 meV for ω_0, and the other control parameters are the same as those employed to depict the band structure shown in Fig. 1 which corresponds to the optimally doped case. The calculation in this case shows that T_c is about 180 K. As seen in Fig. 5 it is found that the gap function has $d_{k_x^2-k_y^2}$-wave symmetry. The $d_{k_x^2-k_y^2}$ symmetry is possible under not only the spin fluctuation mediating pairing but also other anisotropic pairing interactions.[45] We note that the gap function has nodes while it shows finite amplitudes even at the center of the flat region in the electronic structure. This means that the attraction is so strong that the gap function does not

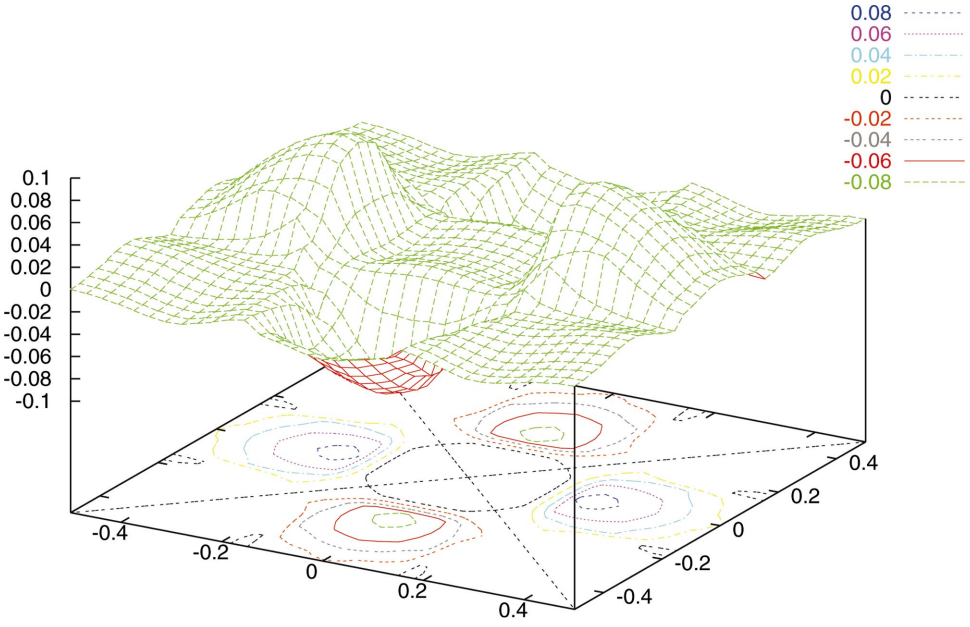

FIG. 5. (Color) A typical example of the superconducting gap function in the wave number space. The x and y directions indicate k_x and k_y, i.e., quasiparticle wave number, respectively, and the z axis gives the amplitude of the gap function. In the numerical calculation, the parameters ω_g, ω_0, K_L, K_T, and λ_L are set to be 13 meV, 64 meV, 0.16, 0.15, and 0.2, respectively. The quasiparticle band structure used is displayed in Fig. 1.

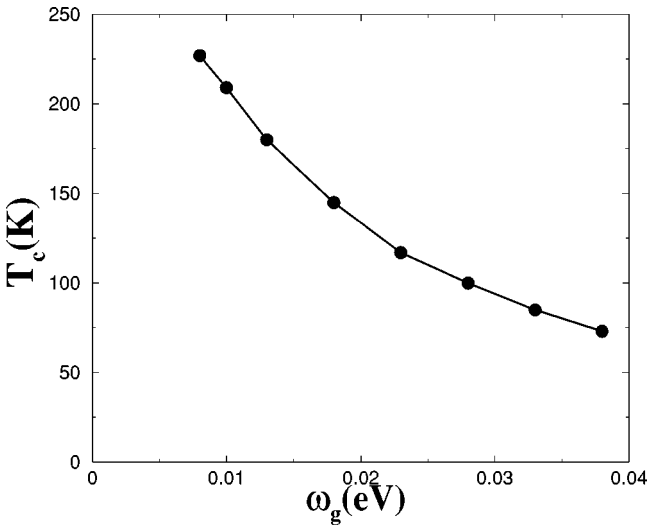

FIG. 6. The ω_g(eV) dependence of T_c (eV). The other paramters are the same as ones used in obtaining Fig. 5.

vanish even in regions except for the Fermi surface. This fact is consistent with the experimental results in ARPES for the optimally doped case showing high T_c.[26] Here, let us explain why the $d_{k_x^2-k_y^2}$ symmetry appears in this case. The gap amplitude is generally dependent on the number density of the interacting quasiparticles and the strength of attraction. Since the number density of the quasiparticles in the flat region is much larger than other regions, the gap function is expected to grow considerably in the flat region. A pair of quasiparticles on the opposite sides of the same flat regions along the $k_x(k_y)$ axis are attracted, while the interaction is repulsive for a pair of quasiparticles belonging to the flat regions that are rotated by 90° relative to each other. Thus, it is found that the gap amplitudes on the different axes should show different signs, resulting in the d symmetry.

As seen in Fig. 6, we found that the value of T_c is nearly inversely related to the depth of the flat region. This tendency is consistent with the experimental results of ARPES,[26] that the depth of the flat region increases with increasing doping and crosses the Fermi level in the overdoped range of composition. At optimum doping, the flat region shows a minimum depth. On the other hand, the value of T_c is dependent also on the width W_{II} of region II, increasing almost linearly with the width. Our calculations show that T_c exceeds 300 K when the value of W_{II} approaches 0.4 with fixing ω_g to be 13 meV, corresponding to optimum doping. It is quite encouraging that such a high value of T_c can be achieved with the present model.

VI. DISCUSSION AND CONCLUSIONS

In this paper the mechanism of high-T_c superconductivity based upon the overscreening of phonons[31,32] was developed further using the results of two recent experimental observations. One is the neutron scattering measurements showing that the frequencies of bond-stretching LO phonons in hole-doped superconducting cuprate oxides being strongly softened in the wave number regions around the Brillouin zone boundaries along the k_x and k_y and that the frequency of the LO phonon is much lower than that of the TO phonons in these regions.[16,19,20,27] This phenomenon is explained in terms of the overscreening of the ionic polarization associated with the LO phonon by phonon-induced charge transfer that results in the negative electronic dielectric function. Another one is the angle-resolved photoemission measurement indicating that in the optimally hole-doped cuprates the flat energy band appears just below the Fermi level around the X (M) points in the Brillouin zone.[26,39] Using the pair interaction derived from the neutron scattering results and the band structure mentioned above, we set up the Eliashberg equation.[31,32] Solving the equation, we observed that the symmetry of the superconducting order parameter is of $d_{k_x^2-k_y^2}$ and the transition temperature is in excess of 200 K under favorable conditions.

The most dominant contribution to the superconducting pairing in the kernel of the Eliashberg equation originates from the phonon contribution that is strongly enhanced by the overscreening effect of the Coulomb interaction. Up to now, several phonon mechanisms leading to the d-wave superconducting gap function due to the anisotropy of the electronic structure have been suggested.[46] In contrast, the present theory relies upon a mechanism of phonon overscreening resulting in the negative electronic dielectric function and strong enhancement of its attractive contribution. As in most of the phonon mechanisms, the present theory predicts that the isotope effect[47] appears in the cuprate superconductors with a relatively low T_c such as LSCO, but this effect may not be visible in the cuprates with a high T_c such as YBCO and Bi-2212, as observed by experiments. This result comes from the fact that as the superconducting transition temperature increases, the pure phonon contribution for the pairing diminishes and the electronic contribution increases instead. This tendency is consistent with the experimental results.[47]

The softening of the LO phonon near the Brillouin zone boundary was observed by neutron scattering even in the superconducting $Ba_{0.6}K_{0.4}BiO_3$ with negligible spin fluctuation[48] and nonsuperconducting $La_{1.69}Sr_{0.31}NiO_4$ (Ref. 49) and $La_{0.7}Sr_{0.3}MnO_3$ (Ref. 50). It appears that the overscreening effect is common in hole-doped transition-metal oxide systems. This phenomenon may be explained in terms of the ''negative Born effective charge,'' which will be further elaborated on later.[37] This concept nicely explains the phonon softening observed for the Peiels-Hubbard Hamiltonian in the one-dimensional Cu-O chain model.[17,18]

In the cuprates the bare bandwidth, calculated, for instance, with the LDA, is of the order of 1 eV. Band narrowing is brought about by spins that almost localize charges and create an extended saddle point in the electronic band structure. In the present paper this effect was considered phenomenologically by using the renormalized band structure. However, a more satisfactory theory should include the quantum effect of spins more explicitly. Using the p-d model hole doping was found to create in-gap states in the Hubbard gap just at the Fermi level, with a dominant oxygen p character.[51] A better model band structure with these features needs to be

developed. A problem here is that we have much less information about the unoccupied states compared to the occupied states, since the photoemission experiments provide information only for the latter, while the inverse-photoemission technique, which should give the information on the former, has much less resolution.

As we mentioned above in the present mechanism LO phonons excite holes from the local oxygen *p* state to the Cu *d* state. The results of inelastic neutron scattering measurements on $YBa_2Cu_3O_{6.95}$ (Ref. 52) suggest that the final state of this transition could be the d_{z^2} level of Cu, since strong mixing of the in-plane Cu-O bond-stretching mode and the apical oxygen mode (62 meV) was observed. This makes the two-band phononic model[53] relevant in the present context. In addition there is a possibility of the transition from an oxygen in the *x* direction to another oxygen in the *y* direction contributing to the *e*-*p* coupling.[54] In the present calculation just one band was assumed for the sake of simplicity, but the reality is likely to be more complex.

Another point that has not been included in the present paper and has to be addressed in future publications is the question of the in-plane anisotropy and the stripe fluctuations. Both the inelastic neutron scattering measurement of the phonon dispersion and the photoemission measurement detected surprisingly strong anisotropy in the CuO_2 plane.[19,20,55,39] This anisotropy most likely is related to the spin-charge phase separation in the form of stripes.[56] While static stripes apparently compete against superconductivity,[58] it is reasonable to assume that the propensity for stripe formation remains strong even in the superconducting phase.[57,16,19,20] The presence of stripes or stripe fluctuations will produce further narrowing of the band and spin-charge interference phenomena, which should enhance the superconductivity. The possibility of such enhancement by confinement, in a more general sense, was emphasized by Phillips.[59] However, since we do not have sufficient information to formulate these phenomena into a rigorous theory, in the present paper we have not explicitly taken them into account. Further experimental as well as theoretical researches are needed to fully account for the spin-charge synergy.

In the present mechanism the role of spins is merely to bring down the energy scale of holes to the level of phonons, so that vibronic resonance can take place. We do not, however, exclude the possibility that the magnetic mechanism also contributes to pairing, at least in some ranges of composition. Even in such a case the phonon mechanism does not compete against the magnetic mechanism because of the *d* symmetry. It is most likely that the relative importance of the phononic and magnetic mechanisms depends upon the charge density; the magnetic mechanism could be more important in the underdoped region, while the phononic mechanism may dominate the optimum and overdoped region.

In the present paper we sacrificed some details as discussed above and greatly simplified the model. Furthermore, it is well known that the calculation of T_c in the Eliashberg theory strongly depends upon details of the parameters. The purpose of this work, therefore, is not to try to describe the superconductivity in the cuprates very accurately, but to demonstrate the possibility of the phononic mechanism of high-T_c superconductivity based upon the overscreening phenomenon. The estimated value of T_c may be even higher than the experimental values over wide ranges of parameters. This is in part due to the fact that the calculation of T_c is essentially based on a mean-field theory and does not include the superconducting fluctuation effect. Inclusion of the fluctuations should significantly decrease T_c, since the pairing force is strong and the system has a two-dimensional nature. The incoherent superconducting fluctuations will be observed as the pseudogap above T_c.

While there are a number of limitations in the present model because of the simplifications and the phenomenological nature, the result described here strongly suggests that the phononic mechanism has to be taken seriously, and careful studies are warranted. At least, the latest experiment indicates that the phononic freedom and the superconducting transition temperature T_c are closely linked since not only the undoped but also the overdoped ones do not show LO phonon softening.[21]

ACKNOWLEDGMENTS

We are indebted to K. A. Müller, A. A. Abrikosov, J. C. Phillips, A. Bussmann-Holder, S. Sachdev, N. Nagaosa, D. Mihailovic, V. V. Kabanov, S. Takahashi, M. R. Norman, N. Hamada, and M. Arai for illuminating discussions. We wish to thank Y. Endoh and J. M. Tranquada for sharing their unpublished experimental results and M.T. especially thanks K. Yamada and J. Mizuki for giving us valuable experimental results prior to publication. Two authors (M.T. and M.M.) were supported by the CREST (JST) project. The other (T.E.) was supported by National Science Foundation Grant No. DMR01-02565. A part of this work was done in Argonne National Laboratory. M.T. and M.M. thank G. Crabtree for his support and M.M. especially thanks A. E. Koshelev for his support and valuable discussions. M.M. also thanks T. Imamura for the offering of a numerical diagonalization program and the staff members of CCSE in JAERI for their computational assistance.

[1] J. G. Bedonorz and K. A. Müller, Z. Phys. B: Condens. Matter **64**, 189 (1986).

[2] See, for example, P. W. Anderson, *The Theory of Superconductivity in the High-Tc Cuprates* (Princeton University Press, Princeton, 1997).

[3] J. Nagamatsu, N. Nakagawa, T. Muranaka, Y. Zenitani, and J. Akimitsu, Nature (London) **410**, 63 (2001).

[4] R. Ricardoda Silva, J. H. S. Torres, and Y. Kopelevich, Phys. Rev. Lett. **87**, 147001 (2001).

[5] C.-T. Chen, P. Seneor, N.-C. Yeh, R. P. Vasquez, L. D. Bell, C. U. Jung, J. Y. Kim, Min-Seok Park, Heon-Jung Kim, and Sung-Ik Lee, Phys. Rev. Lett. **88**, 227002 (2002).

[6] D. J. Scalapino, E. Loh, Jr., and J. E. Hirsh, Phys. Rev. B **34**, 8190 (1986); D. J. Scalapino, Phys. Rep. **250**, 329 (1995), and many references therein.

[7] P. Monthoux and D. Pines, Phys. Rev. B **47**, 6069 (1993); **49**, 4261 (1994). Also, see the recent review, A. V. Chubukov, D. Pines, and J. Schmalian, cond-mat/0201140 (unpublished).

[8] T. Moriya, Y. Takahashi, and K. Ueda, J. Phys. Soc. Jpn. **59**, 2905 (1990).

[9] S. Kambe, H. Yasuoka, A. Hayashi, and Y. Ueda, Phys. Rev. B **47**, 2825 (1993).

[10] H. Sato, A. Tsukada, M. Naito, and A. Matsuda, Phys. Rev. B **62**, R799 (2000).

[11] L. Pintschovius and W. Reichardt, in *Physical Properties of High Temperature Superconductors IV*, edited by D. Ginsberg (World Scientific, Singapore, 1994), p. 295.

[12] T. Egami and S. J. L. Billinge, in *Physical Properties of High Temperature Superconductors V*, edited by D. Ginsberg (World Scientific, Singapore, 1996), p. 265.

[13] H. A. Mook and F. Dogan, Nature (London) **401**, 145 (1999).

[14] A. Lanzara, P. V. Bogdanov, X. J. Zhou, S. A. Keller, D. L. Feng, E. D. Lu, T. Yoshida, H. Eisaki, A. Fujimori, K. Kishio, J.-I. Shimoyama, T. Noda, S. Uchida, Z. Hussain, and Z.-X. Shen, Nature (London) **412**, 510 (2001).

[15] L. Pintschovius, N. Pyka, W. Reichardt, A. Yu. Rumiantsev, N. L. Mitrofanov, A. S. Ivanov, G. Collin, and P. Bourges, Physica C **185-189**, 156 (1991).

[16] R. J. McQueeney, Y. Petrov, T. Egami, M. Yethiraj, G. Shirane, and Y. Endoh, Phys. Rev. Lett. **82**, 628 (1999).

[17] S. Ishihara, T. Egami, and M. Tachiki, Phys. Rev. B **58**, 9485 (1997).

[18] Y. Petrov and T. Egami, Phys. Rev. B **58**, 9485 (1998).

[19] T. Egami, R. J. McQueeney, J.-H. Chung, M. Yethiraj, M. Arai, Y. Inamura, Y. Endoh, S. Tajima, C. Frost, and F. Dogan, Appl. Phys. B (to be published).

[20] T. Egami, J.-H. Chung, R. J. McQueeney, M. Yethiraj, H. A. Mook, C. Frost, Y. Petrov, F. Dogan, Y. Inamura, M. Arai, S. Tajima, and Y. Endoh, Physica B **316-317**, 62 (2002).

[21] K. Yamada and J. Mizuki (private communication). Quite recently, K. Yamada and J. Mizuki *et al.* observed by the x-ray inelastic scattering using synchrotron radiation facilities that the observed LSCO with zero T_c does not show an anomalous softening in the ab-plane bond-stretching LO phonon dispersion.

[22] E.g., J. B. Goodenough and J.-S. Zhou, in *Stripes and Related Phenomena*, edited by A. Bianconi and N. L. Saini (Kluwar Academic, New York, 2000), p. 199.

[23] E.g., T. R. Chien, Z. Z. Wang, and N. P. Ong, Phys. Rev. Lett. **67**, 2088 (1991); C. Kendoriza, D. Mandrus, L. Mihaly, and L. Forro, Phys. Rev. B **46**, 14 293 (1992); A. Carington, A. P. Mackenzie, C. T. Lin, and J. R. Cooper, Phys. Rev. Lett. **69**, 2855 (1992); D. M. Ginzberg, W. C. Lee, and S. E. Stupp, Phys. Rev. B **47**, 12 167 (1993); T. Nishikawa, J. Takeda, and M. Sato, J. Phys. Soc. Jpn. **63**, 1441 (1994); J. Takeda, T. Nishikawa, and M. Sato, Physica C **231**, 293 (1994).

[24] E.g., C. Uher, A. B. Kaiser, E. Gmelin, and I. Waltz, Phys. Rev. B **36**, 5676 (1987); M. Sera and M. Sato, Physica C **185-189**, 1339 (1991); J. L. Cohn, E. F. Skelton, and S. A. Wolf, Phys. Rev. B **45**, 13 140 (1992); Y. Xin, K. W. Wang, C. X. Fan, Z. Z. Sheng, and F. T. Chang, *ibid.* **48**, 557 (1993).

[25] There are many references. For NMR, see N. J. Curro, T. Imai, C. P. Slichter, and B. Dabrowski, Phys. Rev. B **56**, 877 (1997); G. Aeppli, T. E. Mason, S. M. Hayden, H. A. Mook, and J. Kulda, Science (Washington, DC, U.S.) **278**, 1432 (1997). For ARPES, see A. G. Loeser, Z.-X. Shen, D. S. Dessau, D. S. Marshall, C. H. Park, P. Fournier, and A. Kapitulnik, *ibid.* **273**, 325 (1996); H. Ding, T. Yokoya, J. C. Campuzano, T. Takahashi, M. Randeria, M. R. Norman, T. Mochiku, K. Kadowaki, and J. Giapintzakis, Nature (London) **382**, 51 (1996). For tunneling, see Ch. Rener, B. Revaz, J.-Y. Genoud, K. Kadowaki,and O. Fischer, Phys. Rev. Lett. **80**, 149 (1998).

[26] E.g., for LSCO, see A. Ino, C. Kim, M. Nakamura, T. Yoshida, T. Mizokawa, A. Fujimori, Z.-X. Shen, T. Kakeshita, H. Eisaki, and S. Uchida, Phys. Rev. B **65**, 094504 (2002). For YBCO, see D. H. Lu, D. L. Feng, N. P. Armitage, K. M. Shen, A. Damascelli, C. Kim, F. Ronning, Z.-X. Shen, D. A. Bonn, R. Liang, W. N. Hardy, A. I. Rykov, and S. Tajima, Phys. Rev. Lett. **86**, 4370 (2001). For Bi-2212, see M. R. Norman, H. Ding, M. Randeria, J. C. Campuzano, T. Yokoya, T. Takeuchi, T. Takahashi, T. Mochiku, K. Kadowaki, P. Guptasarma, and D. G. Hinks, Nature (London) **392**, 157 (1998).

[27] J.-H. Chung, T. Egami, R. J. McQueeney, M. Yethiraj, M. Arai, T. Yokoo, Y. Petrov, H. A. Mook, Y. Endoh, S. Tajima, C. Frost, and F. Dogan (unpublished).

[28] V. L. Ginzburg and D. A. Kizhnits, *High Temperature Superconductivity* (Consultants Bureau, New York, 1976).

[29] C. C. Tsuei *et al.*, Phys. Rev. Lett. **73**, 593 (1994). For a review of the experiments, see D. J. van Harilingen, Rev. Mod. Phys. **67**, 515 (1995); for the theoretical aspects, see D. J. Scalapino, Phys. Rep. **250**, 329 (1995), and references therein.

[30] E.g., S. Uchida, T. Ido, H. Takagi, T. Arima, Y. Tokura, and S. Tajima, Phys. Rev. B **43**, 7942 (1991).

[31] M. Tachiki and S. Takahashi, Phys. Rev. B **38**, 218 (1988).

[32] M. Tachiki and S. Takahashi, Phys. Rev. B **39**, 293 (1989).

[33] M. Tachiki, Curr. Appl. Phys. (to be published).

[34] T. Egami, S. Ishihara, and M. Tachiki, Science **261**, 1307 (1993).

[35] R. Resta, Rev. Mod. Phys. **66**, 899 (1994).

[36] R. D. King-Smith and D. Vanderbilt, Phys. Rev. B **47**, 1651 (1993).

[37] P. Piekarz, T. Egami, and M. Tachiki (unpublished).

[38] D. A. Krizthnits, E. G. Maksimov, and D. I. Khomskii, J. Low Temp. Phys. **10**, 79 (1973).

[39] In this paper, we especially focus on ARPES and inelastic neutron scattering in YBCO because both data are now available for its optimum doped one. For ARPES in YBCO, see D. H. Lu, D. L. Feng, N. P. Armitage, K. M. Shen, A. Damascelli, C. Kim, F. Ronning, Z.-X. Shen, D. A. Bonn, R. Liang, W. N. Hardy, A. I. Rykov, and S. Tajima, Phys. Rev. Lett. **86**, 4370 (2001).

[40] There are many references. For the Hubbard model, see N. Bulut, D. J. Scalapino, and S. R. White, Phys. Rev. B **50**, 7215 (1994); E. Dagotto, Rev. Mod. Phys. **66**, 763 (1994). For recent calculations, see S. Onoda and M. Imada, cond-mat/0108416 (unpublished); Y. Saiga and M. Imada, cond-mat/0110458 (unpublished). For the t-J model, see E. Dagotto and A. Nazarenko, Phys. Rev. Lett. **73**, 728 (1994), and for recent calculations, see A. Himeda and M. Ogata, *ibid.* **85**, 4345 (2000).

[41] N. Hamada (private communication).

[42] M. Machida, M. Tachiki, and T. Egami (unpublished).

[43] C. C. Homes, A. W. McConnell, B. P. Clayman, D. A. Bonn, R. Liang, W. N. Hardy, M. Inoue, H. Negishi, P. Fournier, and R. L.

Greene, Phys. Rev. Lett. **84**, 5391 (2000).
[44] E. A. Pashitskii, V. I. Pentegov, A. V. Semenov, and L. Abraham, JETP Lett. **69**, 753 (1999); E. A. Pashitskii and V. I. Pentegov, *ibid.* **72**, 439 (2000).
[45] See, e.g., A. Sherman, Phys. Rev. B **55**, 582 (1997).
[46] See, e.g., A. A. Abrikosov, Physica C **336**, 163 (2000); Phys. Rev. B **63**, 134518 (2001).
[47] For recent experimental data, see G. Zhao, V. Kirtikar, and D. E. Morris, Phys. Rev. B **63**, 220506 (2001) and references therein.
[48] M. Braden, W. Reichardt, E. Elkaim, J. P. Lauriat, S. Shiryaev, and S. N. Barilo, Phys. Rev. B **62**, 6708 (2000); M. Braden, W. Reichardt, S. Shiryaev, and S. N. Brilo, cond-mat/0107498 (unpublished).
[49] L. Pintschovius, W. Reichardt, M. Braden, G. Dhalenne, and A. Revcolevchi, Phys. Rev. B **64**, 094510 (2001); J. M. Tranquada, K. Nakajima, M. Braden, L. Pintschovius, and R. J. McQueeney, Phys. Rev. Lett. **88**, 075505 (2002).
[50] W. Reichardt and M. Braden, Physica B **263-264**, 416 (1998).
[51] E.g., S. Ishihara, H. Matsumoto, S. Odashima, M. Tachiki, and F. Mancini, Phys. Rev. B **49**, 1350 (1994).
[52] J.-H. Chung, T. Egami, R. J. McQueeney, M. Yethiraj, M. Arai, T. Yokoo, H. A. Mook, Y. Endoh, S. Tajima, C. Frost, and F. Dogan (unpublished).
[53] A. Bussmann-Holder, K. A. Müller, R. Micnas, H. Büttner, A. Simon, A. R. Bishop, and T. Egami, J. Phys.: Condens. Matter **13**, L169 (2001).
[54] D. Mihailovic and V. V. Kabanov, Phys. Rev. B **63**, 054505 (2001).
[55] L. Pintshovius, J. M. Tranquada, and Y. Endoh (private communication).
[56] J. M. Tranquada, D. J. Buttrey, V. Sachan, and J. E. Lorenzo, Phys. Rev. Lett. **73**, 1003 (1994); J. M. Tranquada, B. J. Sternlieb, J. D. Axe, Y. Nakamura, and S. Uchida, Nature (London) **375**, 561 (1995); J. M. Tranquada, J. D. Axe, N. Ichikawa, A. R. Moodenbauch, Y. Nakamura, and S. Uchida, Phys. Rev. Lett. **78**, 338 (1997).
[57] K. Yamada, C. H. Lee, K. Kurahashi, J. Wada, S. Wakimoto, S. Ueki, H. Kimura, Y. Endoh, S. Hosoya, G. Shirane, R. J. Birgeneau, M. Greven, M. A. Kastner, and Y. J. Kim, Phys. Rev. B **57**, 6165 (1998); A. W. Hunt, P. M. Singer, K. R. Thurber, and T. Imai, Phys. Rev. Lett. **82**, 4300 (1999); X. J. Zhou, P. Bogdanov, S. A. Kellar, T. Noda, H. Eisaki, S. Uchida, Z. Hussain, and Z.-X. Shen, Science (Washington, DC, U.S.) **286**, 268 (1999); M. Fujita, K. Yamada, H. Hiraka, P. M. Gehring, S. H. Lee, S. Wakimoto, and G. Shirane, Phys. Rev. B **65**, 064505 (2002).
[58] J. M. Tranquada, J. D. Axe, N. Ichikawa, Y. Nakamura, S. Uchida, and B. Nachumi, Phys. Rev. B **54**, 7489 (1997).
[59] J. C. Phillips, Proc. Natl. Acad. Sci. U.S.A. **94**, 12771 (1997).